



HAL
open science

Towards the Detection of High-Contrast Cs CPT Resonances Using a Single Modulated Diode Laser

X. Liu, E. Kroemer, J.-M. Merolla, R. Boudot

► **To cite this version:**

X. Liu, E. Kroemer, J.-M. Merolla, R. Boudot. Towards the Detection of High-Contrast Cs CPT Resonances Using a Single Modulated Diode Laser. European Frequency and Time Forum, Apr 2012, Gothenburg, Sweden. pp.3, 10.1109/EFTF.2012.6502388 . hal-00744636

HAL Id: hal-00744636

<https://hal.science/hal-00744636>

Submitted on 15 Apr 2021

HAL is a multi-disciplinary open access archive for the deposit and dissemination of scientific research documents, whether they are published or not. The documents may come from teaching and research institutions in France or abroad, or from public or private research centers.

L'archive ouverte pluridisciplinaire **HAL**, est destinée au dépôt et à la diffusion de documents scientifiques de niveau recherche, publiés ou non, émanant des établissements d'enseignement et de recherche français ou étrangers, des laboratoires publics ou privés.



Distributed under a Creative Commons Attribution 4.0 International License

Towards the Detection of High-Contrast Cs CPT Resonances Using a Single Modulated Diode Laser

X. Liu, E. Kroemer, J. M. Merolla, R. Boudot

Abstract—This paper reports the key development steps of a Bi-Frequency Bi-Polarization (BiFBiP) laser system that generates from a single externally-modulated Distributed Feedback (DFB) laser source two phase-coherent optical lines resonant on the Cs D_1 line (894.6 nm), frequency-split by 9.192 GHz and exhibiting linear crossed polarizations. Two different architectures, based on electro-optic modulators as key components for optical sidebands generation, are presented. Residual frequency stability performances of the DFB laser source are measured to be less than 10^{-11} for integration times up to 200 s. Phase noise performances of the optically carried microwave signal as well as polarization analysis at the output of the BiFBiP system are reported. Using this laser system, Coherent Population Trapping (CPT) resonances with contrast up to 5.8 % in a mm-scale vapor cell and 22 % in a cm-scale cell are preliminary reported.

I. INTRODUCTION

A major drawback of traditional vapor cell clocks based on Coherent Population Trapping (CPT) [1] is the detection of the atomic clock resonance with a poor contrast (about 1 %). This is partly due in standard CPT clocks to the use of a circular polarization excitation scheme leading numerous atoms to be lost in extreme Zeeman sub-levels. Different optimized CPT pumping schemes were proposed to maximize the number of atoms participating to the clock 0-0 transition and consequently increase dramatically the CPT resonance contrast. Y. Jau et al. proposed the so-called push-pull interaction scheme where atoms interact with a D_1 line resonant bi-chromatic optical field that alternates between right and left circular polarization at the Bohr frequency of the state [2]. Contrasts up to 30 % were reported with this method. A method based on the use of a $\sigma_+ - \sigma_-$ configuration of polarized counterpropagating waves resonant with D_1 line of alkali metal atoms in small-size cells was proposed in [3]. Later, the same group proposed the *lin par lin* method and experimentally demonstrated the possibility to increase significantly the contrast of dark resonances on the D_1 line of alkali atoms with nuclear spin $I = 3/2$ using bichromatic linearly polarized light [4]. A prototype atomic clock based on *lin||lin* coherent population trapping resonances in Rb atomic vapor was developed in [5]. This method was more recently implemented with alkali atoms of large nuclear spin (Cs atom : $I = 7/2$) and demonstrated CPT contrasts of about 10 % [6]. In 2007, V. Shah et al. demonstrated an alternative method to produce very high-contrast CPT resonances by using four-wave mixing in ^{87}Rb atoms [7]. T. Zanon et al. demonstrated the detection of increased CPT resonance contrasts with a so-called *lin per lin* interaction scheme

using two linear orthogonally polarized optical lines [8]. CPT contrasts higher than 50 % was obtained using this technique [9]. Nevertheless, this method was demonstrated with two phase-locked lasers. This induces a complex experimental set-up with two laser sources, independent laser electronics, multiple optics components and a low noise optical phase lock-loop. Recently, efforts have been done in different groups and different experimental schemes have been proposed to realize this *lin per lin* interaction scheme with a single laser source [10], [11]. Both of these last articles report research studies based on Rb atom.

The present article aims to report first development steps of a Bi-Frequency Bi-Polarization (BiFBiP) laser system that generates with a single externally-modulated Distributed Feedback (DFB) laser source two phase-coherent optical lines resonant on the Cs D_1 line, frequency-split by 9.192 GHz with linear crossed polarizations. This system is constructed in order to allow the detection of high-contrast Cs CPT resonances through the *lin per lin* interaction scheme. Key components used for light field modulation are pigtailed pigtailed LiNbO_3 electro-optic modulators (EOMs). Two different architectures are proposed, including one inspired from [10]. Preliminary results report CPT contrasts up to 20 % in Cs vapor cm-scale cells.

II. FREQUENCY-STABILIZED DISTRIBUTED FEEDBACK LASER SOURCE

A frequency-stabilized laser diode is required in the BiFBiP system. Narrow-linewidth extended cavity diode lasers (ECDLs) are usually used for this purpose [12], [13], [14], [15]. Nevertheless, such laser sources require high immunity to ambient vibrations, optical misalignment and accurate control of the cavity length. Nowadays, Distributed Feedback (DFB) lasers represent an efficient and simple alternative when narrow linewidth is desired.

In our BiFBiP system, the laser source is a commercially available GaAs semiconductor distributed feedback laser diode with integrated grating structure emitting in a single-mode at 895 nm. It is housed in a hermetic TO-3 package with thermistance and thermoelectric cooler. It is driven by a low noise current controller inspired from [16]. The DFB laser is frequency-stabilized using standard saturated absorption technique. The feedback correction is applied to the laser current with a servo bandwidth of about 500 Hz. Fig. 1 shows the DFB laser setup. Further details are reported in [17].

Two similar laser systems have been developed to evaluate the laser relative frequency stability. Figure 2 shows the Allan deviation of the beatnote signal frequency between both lasers in free running and locked conditions.

The authors are with FEMTO-ST, CNRS, 26 chemin. de l'Épitaphe, Besançon, France. e-mail: {rodolphe.boudot}@femto-st.fr

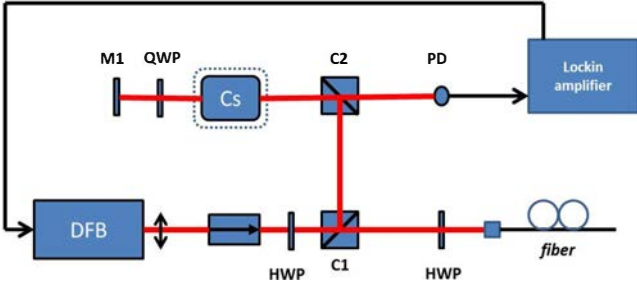


Fig. 1. Distributed Feedback laser diode optical set-up. QWP : quarter-wave plate, HWP : half-wave plate, PD : photodiode, M1 : mirror, C1 and C2 : polarizing cube splitters, Cs : Cs cell.

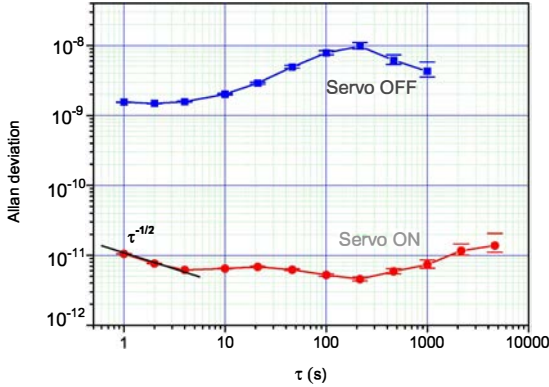


Fig. 2. Allan deviation of the DFB laser beatnote frequency (servo ON or servo OFF).

In the free-running regime, the frequency stability is measured to be 1.5×10^{-9} at 1 s. In the stabilized regime, it is 1×10^{-11} at 1 s. The Allan deviation decreases as a white frequency noise during a few seconds before reaching a wide flicker floor at about 5×10^{-12} . For integration times longer than 200 s, the laser frequency stability is slowly degraded. These results compare favorably with those presented in [18], [19] on Cs D₂ line and are greatly satisfying for a CPT Cs atomic clock.

III. BiFBiP ARCHITECTURES

A. Architecture 1

Fig. 3 shows a simplified scheme of the BiFBiP architecture 1.

The laser output beam is splitted into two parallel arms using a polarizing cube splitter. A half-wave plate is placed before the cube to separate the incident beam into two orthogonal polarization axes with equal power. In the first arm, a pigtailed Mach-Zehnder EOM (MZ EOM) is used to generate two in-phase optical sidebands separated from the carrier by the modulation frequency. The dc electrode bias voltage of the MZ EOM is adjusted in order to obtain three optical lines of equal amplitude. In the other arm, a phase pigtailed EOM allows to generate two optical sidebands around the carrier, each of them with opposite phase. Both arms are then recombined using a polarizing cube combiner.

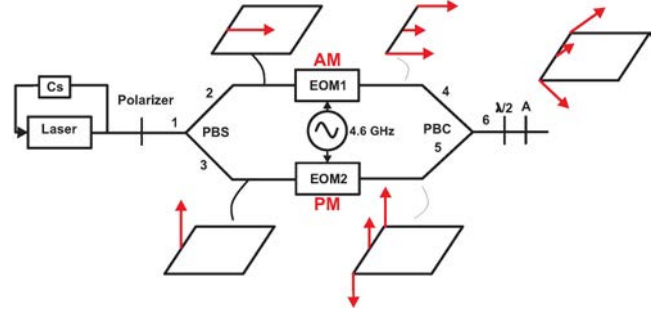


Fig. 3. Architecture 1 : 2 EOMs (a phase EOM and an amplitude MZ EOM) are placed into two parallel arms. The modulation frequency can be 9.192 GHz or 4.596 GHz.

At the BiFBiP output, the carrier is found to be parallel with the first sideband while it is orthogonally polarized to the second optical sideband. In this architecture, the laser can be modulated either at 9.192 GHz or 4.596 GHz. In the first case, CPT interaction will occur thanks to the optical carrier and one sideband. In the second case, CPT interaction is realized using both optical sidebands. Both EOMs, including their fiber input and output, are actively temperature-controlled and placed in a box containing insulating foam. In this architecture, the output spectrum is mainly composed here by three optical lines. Only two of them participate to the CPT interaction. Up to date, no selective optical filter has been placed at the output of the system to suppress the spurious sideband. This will be implemented in a near future.

B. Architecture 2

The second architecture (4) is inspired by and well described in [10].

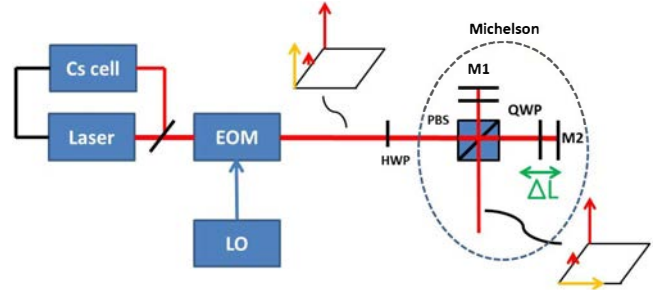


Fig. 4. Architecture 2 : CPT sidebands are generated using a pigtailed MZ EOM driven at 4.596 GHz. The EOM dc electrode bias voltage is tuned to suppress the optical carrier. The best carrier rejection is measured to be 37 dB. Both optical lines are separated and orthogonally polarized using a phase-imbalanced Michelson interferometer.

A MZ EOM, driven at 4.596 GHz, is used to generate two optical sidebands separated of 9.192 GHz from the carrier. The EOM transfer function bias point is stabilized to the so-called dark point where the optical carrier is optimally suppressed using a microwave technique similar to the one described in [20]. A typical carrier rejection of 37 dB is obtained. At the output of the EOM, a Michelson interferometer is placed to separate optical lines and orthogonally polarize them. It is shown that both optical lines of frequency f_1 and f_2 incident

on the cube are orthogonally polarized at the output of the cube if the phase differences satisfy the relations :

$$2k_1\Delta L = 2m\pi \quad (1)$$

$$2k_2\Delta L = 2(n+1)\pi \quad (2)$$

where m and n are integers, $2\Delta L$ is the optical path difference between the two arms and k_1 , k_2 are wavevectors for the fields f_1 and f_2 respectively.

It can then be found that the condition required to obtain linear crossed polarizations at the output of the cube is :

$$\Delta L = \frac{c}{4\Delta f} \quad (3)$$

In the case of the Cs atom ($\Delta f = f_2 - f_1 = 9.192$ GHz), we obtain $\Delta L = 8.15$ mm.

In such a scheme, changes in the phase difference $\varphi_1 = 2k_1\Delta L$ are caused by changes of f_1 and ΔL such that $\delta\varphi_1 = \frac{\pi\delta f_1}{\Delta f}$ and $\delta\varphi_1 = \frac{4\pi\delta(\Delta L)}{\lambda_1}$ respectively with λ_1 the field wavelength. For a Rb CPT experiment, authors in [10] report that a delicate control of the experiment such that $\delta f_1 < 190$ MHz et $\delta(\Delta L) < 12$ nm must be achieved to optimize the behavior of the system. The first condition is easily reached with a laser frequency stabilization based on saturated absorption technique. The second condition requires careful temperature control of the Michelson interferometer ensemble. The use of free-space discrete components has been preferred for the Michelson interferometer. Total dimensions are minimized to limit sources of optical length fluctuations.

IV. TECHNOLOGIES AND CHARACTERIZATION OF THE BiFBiP SYSTEM

A. A low phase noise 9.192 GHz local oscillator

CPT sidebands are achieved in the BiFBiP system by modulating at 9.192 GHz or 4.596 GHz electro-optic modulators. For this purpose, we developed (see Fig. ??) low phase noise Non-Linear Transmission Line (NLTL)-based 9.192 GHz frequency synthesizers driven by a high-performance 5 MHz quartz-crystal oscillator. The multiplication process from 5 MHz to 9.192 GHz is similar to the one described in [21]. The only slight difference stands for the use of Gali-84+ amplifiers at the output of the 100-200 MHz doublers. These amplifiers are low-power consumption and easy-to-use devices. They can exhibit a 22-25 dBm output power allowing to drive and saturate NLTLs correctly. A low-noise frequency divider by 10 is typically used at the output of the synthesis when a 4.596 GHz signal is required.

Fig. 5 reports the residual phase noise of the frequency synthesizers at 100 MHz and 9.192 GHz. Phase noise performances for two synthesizers at 9.192 GHz are -75 dBrad²/Hz, -105 dBrad²/Hz and -113 dBrad²/Hz at 1 Hz, 1 kHz and 10 kHz offset frequencies respectively.

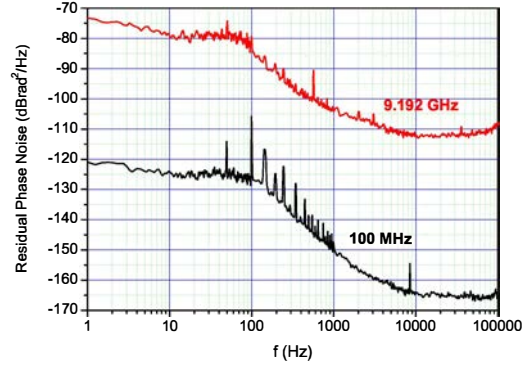


Fig. 5. Residual phase noise of frequency synthesizers at 100 MHz and 9.192 GHz.

B. Phase noise of the optically carried 9.192 GHz signal

Atoms in the cell interact with the optically carried 9.192 GHz signal from the BiFBiP system. It is then required to verify that the microwave signal phase noise is not degraded through optic transfer. For this purpose, the measurement set-up described in 6 was implemented to characterize the residual phase noise at 9.192 GHz of the optically carried signal.

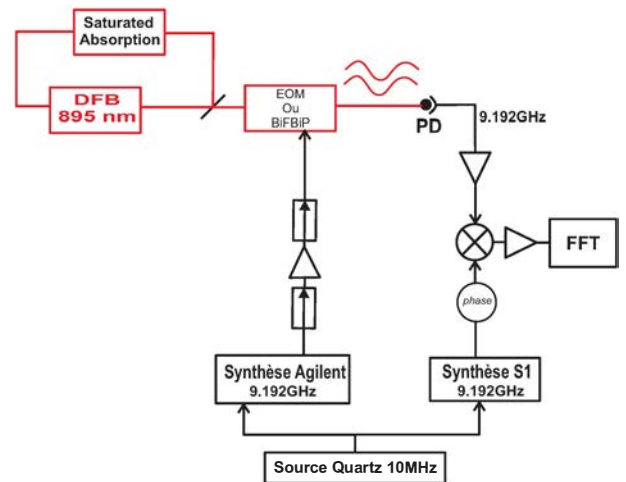


Fig. 6. Residual phase noise measurement set-up to characterize performances of the optically carried 9.192 GHz signal at the output of the BiFBiP system.

A common quartz-oscillator reference is splitted into two arms and drives two microwave synthesizers. The commercial synthesizer is used to drive at 9.192 GHz the EOM in the BiFBiP system. At the output of the BiFBiP system, the 9.192 GHz modulation signal is detected by a fast photodiode, amplified by a low-noise microwave amplifier and bandpass filtered (filter bandwidth ~ 50 MHz) (not visible in the figure). Microwave isolators are inserted to prevent microwave feedback and optimize impedance matching. This signal is phase-compared to the 9.192 GHz signal from the second synthesizer using a saturated microwave mixer. The latter operates as a phase detector. The mixer output voltage is analysed using a FFT analyser.

Fig. 7 reports the residual phase noise performances at 9.192 GHz for the BiFBiP architecture 2. Note that all these measurements are strictly limited by the residual phase noise performances of the Agilent E8254A commercial synthesizer. It is pointed out that there is no phase noise degradation between the direct output of the NLTL-based frequency synthesizer and the output of the complete BiFBiP system.

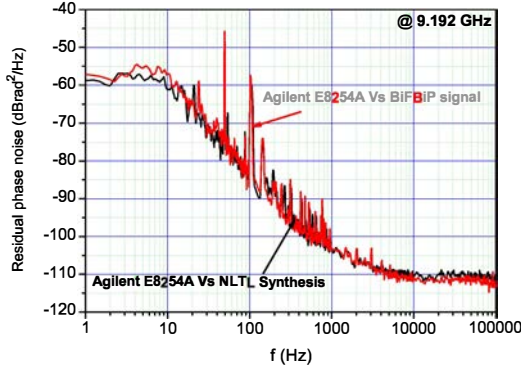


Fig. 7. Residual phase noise at 9.192 GHz of the NLTL-based synthesizer and of the optically carried 9.192 GHz signal at the output of the BiFBiP system (architecture 2).

C. Analysis of polarization

We checked the ability to generate two linearly crossed optical lines at the output of the BiFBiP structure by placing a linear analyser at its output. Fig. 8 reports the evolution of optical power in both optical lines versus the analyser angle (case of BiFBiP architecture 2). It is demonstrated that both optical lines at the output of the system are orthogonally polarized. For both axes, the minimum of transmission is close to be zero. This proves that both fields are really linearly polarized along orthogonal directions. The difference in amplitude is due to the fact that both photodiodes did not present exactly the same transimpedance gain. We confirm that orthogonally polarized optical lines have also been obtained in the case of the BiFBiP architecture 1.

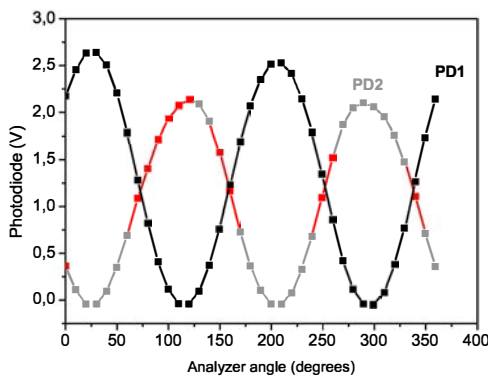


Fig. 8. Voltage at the output of both photodiodes (image of laser power) versus the analyser angle. Case of the BiFBiP architecture 2.

V. PRELIMINAR DETECTION OF CPT RESONANCES

This section is devoted to report Coherent Population Trapping resonances detected in Cs vapor cells. Two cells have been tested. Both of them are filled with a buffer gas to operate in the Dicke regime [22]. The first cell is a 2-mm diameter and 1.4 mm-length microfabricated cell realized according to the process described in [23]. This cell is filled with a Ne pressure of 75 Torr. The second cell is a 5-cm long and 2-cm diameter pyrex cell with a N₂-Ar buffer gas mixture. The total pressure is 15 Torr with a pressure ratio $r = P(Ar)/P(N_2) = 0.4$. For the detection of CPT resonances in correct conditions, cells are temperature-controlled, surrounded by a static magnetic field of a few μT and placed in a double layer mu-metal magnetic shield to prevent external electromagnetic perturbations.

A. Architecture 1

Figs 9(a) and 9(b) report a Zeeman spectrum detected in the microcell heated at 80°C for two different CPT excitation schemes.

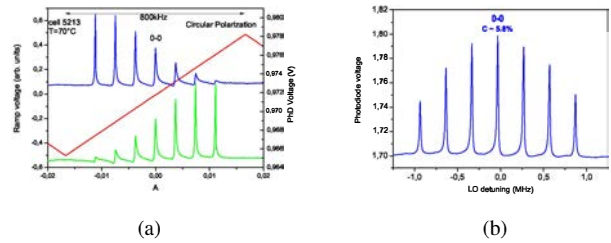


Fig. 9. Zeeman spectrum obtained in microfabricated cell (Cs-Ne 75 Torr) heated at 80°C. (a) : Circular polarization in σ^+ or σ^- configuration (b) : BiFBiP laser. The modulation frequency is 9.192 GHz.

In the first case, atoms interact with circularly polarized light (standard technique in CPT clocks). Zeeman sublevels with the angular momentum projection $m = \pm 3$ are favored. In the second case, atoms interact with light coming from the BiFBiP laser. The total resonant laser power is about the same in both cases. While extreme Zeeman sublevels are favorably populated in the circular polarization excitation scheme, it is clearly pointed out that the clock 0-0 transition is optimized with the BiFBiP system. The contrast of the 0-0 resonance, defined as the ratio between the CPT signal height and the background, is measured to be 5.8% with the BiFBiP system whereas it is only 1.7% in the classical configuration. This represents a improvement factor of 3.4.

B. Architecture 2

Figs 10(a) and 10(b) show a Zeeman spectrum and a zoom on the clock 0-0 resonance respectively detected in the cm-scale Cs-N₂-Ar. The cell is heated at 33°C. The laser beam incident on the cell is only 6-mm diameter.

It is noted that the Zeeman spectrum presents a clear symmetry. The 0-0 transition contrast is 21.4 %. These results should be improved with an increased laser intensity up to a saturation value, a proper adjustment of the cell temperature [24] or a bigger beam diameter to make participate a maximum

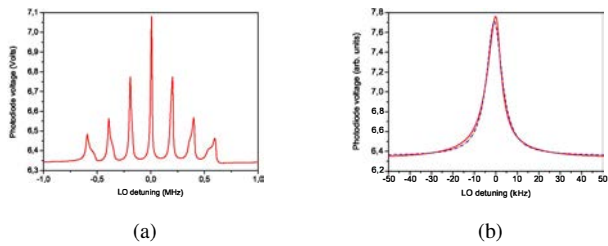


Fig. 10. (a) Zeeman spectrum. The deformation of Zeeman lines is due to the fact that the static magnetic field is not well homogeneous along the whole length of the cell. The cell was inserted in a physics package devoted to be used with cells of maximum length 2 cm. (b) : Zoom on the 0-0 resonance. The contrast is 21.4 %. The total laser power is 800 μ W.

number of atoms to the CPT interaction. Nevertheless, these results remain very encouraging. Detailed characterizations of CPT resonances with BiFBiP architectures versus several experimental parameters will be led in a near future.

VI. CONCLUSIONS

We demonstrated the detection of high-contrast CPT resonances in Cs vapor cells using a single modulated laser source that generates at 895 nm two optical lines frequency-separated by 9.192 GHz with linear crossed polarizations. A frequency-stabilized DFB laser source with a relative frequency stability better than 10^{-11} for integration times up to 1000 s was developed. Two different so-called BiFBiP architectures based on electro-optic modulators have been tested. Low phase noise 9.192 frequency synthesizers were developed to drive EOMs. Residual phase noise performances of optically carried 9.192 GHz signal at the output of the BiFBiP system was evaluated. CPT resonance clock (0-0) transition with contrast of 5.8 % was reported in a Cs-Ne mm-scale cell with the architecture 1. In a cm-scale cell, CPT contrasts up to 21 % were reported with the architecture 2.

ACKNOWLEDGMENTS

This study was realized in the frame of a contract with Laboratoire National de métrologie et d'Essais (LNE). This work was partly funded by Région de Franche-Comté. X. Liu PhD thesis is supported by Région de Franche-Comté. We thank Philippe Abbé (FEMTO-ST) for technical support in electronics and mechanics design, E. Rubiola and V. Giordano (FEMTO-ST) for their help about the MZ EOM microwave stabilization technique, E. De Clercq (LNE-SYRTE) for fruitful discussions about optimized CPT pumping schemes. The authors wish to express their gratitude to S. Guérandel (LNE-SYRTE) for lending us the Cs-N₂-Ar cm-scale cell.

REFERENCES

[1] J. Vanier, *Appl. Phys. B*, **81**, pp 421-442 (2005).
 [2] Y. Y. Jau, E. Miron, A. B. Post, N. N. Kuzma and W. Happer, *Phys. Rev. Lett.*, **94**, (16), 160802 (2004).
 [3] A. V. Taichenachev, V. I. Yudin, V. L. Velichansky, S. V. Kargapoltsev, R. Wynands, J. Kitching and L. Hollberg, *JETP Lett.*, **80**, (4), 236 (2004).
 [4] A. V. Taichenachev, V. I. Yudin, V. L. Velichansky and S. A. Zibrov, *JETP Lett.*, **82**, (7), 398 (2005).

[5] E. E. Mikhailov, T. Horrom, N. Belcher, and I. Novikova, *J. Opt. Soc. Am. B*, **27**, pp 417-422 (2010).
 [6] K. Watabe, T. Ikegami, A. Takamizawa, S. Yanagimachi, S. Ohshima and S. Knappe, *Applied Opt.*, **48**, (6), 1098 (2009).
 [7] V. Shah, S. Knappe, L. Hollberg and J. Kitching, *Opt. Lett.*, **32**, (10), 1244 (2007).
 [8] T. Zanon, S. Guérandel, E. de Clercq, D. Holleville, N. Dimarcq and A. Clairon, *Phys. Rev. Lett.*, **94**, 193002, (2005).
 [9] N. Castagna, R. Boudot, S. Guérandel, E. De Clercq, N. Dimarcq and A. Clairon, *IEEE Trans. Ultrason. Ferroelec. Freq. Contr.*, **56**, (2), pp 246-253 (2009).
 [10] S. H. Yim et al., *Rev. Sci. Instr.* **79**, 126104 (2008).
 [11] P. Yun et al., *Rev. Sci. Instr.* **82**, 123104 (2011).
 [12] G. D. Rovera, G. Santarelli and A. Clairon, *Rev. Sci. Instrum.* **65**, 5, 1502-1505 (1994).
 [13] C. Affolderbach and G. Mileti, *Optics and Lasers in Engineering* **43**, 291-302 (2005).
 [14] C. Affolderbach and G. Mileti, *Rev. Sci. Instr.* **76**, 073108 (2005).
 [15] X. Baillard, A. Gauguet, S. Bize, P. Lemonde, P. Laurent, A. Clairon and P. Rosenbusch, *Opt. Comm.* **266**, 609-613 (2006).
 [16] K. G. Libbrecht and J. L. Hall *Rev. Sci. Instr.* **64**, 8, 2133-2135 (1993).
 [17] X. Liu and R. Boudot *IEEE Trans. Instr. Meas.*, to be published (2012).
 [18] F. Bertinetto, P. Cordiale, G. Galzerano and E. Bava, *IEEE Trans. Instr. Meas.* **50**, 2, 490-492 (2001).
 [19] T. Hori, A. Araya, S. Moriwaki and N. Mio, *Rev. Sci. Instrum.* **78**, 026105 (2007).
 [20] B. Onillon, P. Danes, B. Benazet and O. Llopis, *Microwave and Opt. Tech. Lett.*, **49**, 7, 1634 (2007).
 [21] R. Boudot, S. Guérandel and E. De Clercq, *IEEE Trans. Instr. Meas.*, **58**, 10, 3659-3665 (2009).
 [22] R. H. Dicke, *Phys. Rev.* **89**, 472 (1953).
 [23] M. Hasegawa, R. K. Chutani, C. Gorecki, R. Boudot, P. Dziuban, V. Giordano, S. Clatot, L. Mauri, *Sensors Actuat. A : Phys.*, **167**, 594 (2011).
 [24] S. Knappe, R. Wynands, J. Kitching, H. G. Robinson and L. Hollberg *Journ. Opt. Soc. Am. B* **18**, 1545 (2001).